MedCrave
Step into the World of Research
Journal of Analytical & Pharmaceutical research

Research Article
Open Access
CrossMark

Equilibrium and kinetic behavior of Pb(II) ions sorption onto thermally treated clay-rich soil collected near Gelemso town of Oromia region in Ethiopia

Abstract

Equilibrium and kinetic studies of Pb (II) ions sorption onto a thermally treated clay-rich soil, collected from a site (8.822634N, 40.523574E) near Gelemso town in Western Hararghie Zone of Oromia region of Ethiopia, have been carried out by batch experiments. The sorption equilibrium data analyzed in the light of Langmuir-, Freundlich-, and Temkin isotherms showed that the Freundlich isotherm represents the best fit for the experimental data. For revealing the mechanism of Pb (II) ions sorption onto the studied sorbent, the observed data was analyzed in terms of pseudo-first-order, pseudo-second-order, intra-particle diffusion, Boyd, and Elovich Kinetic Models. The pseudo-second-order kinetic model with the high correlation coefficient (R^2) predicted sorption capacity closer to the experimental value. With Pb(II) initial concentration 20 mg L^{-1}, and optimized adsorbent dose and pH, as high as 95% Pb(II) ions could be removed within 3 hrs. Therefore, the studied clay-rich soil can be used as a low-cost and efficient alternative sorbent, for the large scale treatment of wastewater contaminated with Pb (II) ions.

Keywords: chemisorption, intra-particle, diffusion, equilibrium, isotherms

Volume 11 Issue 2 - 2022

Abraham Fikre, Tesfahun Kebede, OP Yadav
Chemistry Department, Haramaya University, Ethiopia

Correspondence: OP Yadav, Chemistry Department, Haramaya University, Ethiopia, Email yadavop02@yahoo.com

Received: April 11, 2022 | **Published:** June 30, 2022

Introduction

The increasing establishment of industries manufacturing various agrochemicals, petrochemicals and diverse *anthropogenic* activities have led to the pollution of our environment with diverse hazardous chemicals including heavy metals.[1,2] Most of the global surface water contaminated with heavy metals has become a serious health problem for living bodies. The hazardous substances including heavy metals present in wastewater endanger the public health as well as aquatic organisms. Additionally, heavy metals-loaded untreated effluents released from some industries degrade the agricultural land causing a diminished crops yield.

The lead poisoning due to the intake of lead-contaminated food, water and air is of major public health problem mainly in developing countries. In particular, the presence of highly toxic lead in water or food material is directly associated with health risk such as damage to liver, kidney, reproductive and central nervous systems. The quantum of lead intake is influenced by the age and behavioral characteristics of the individual and the bioavailability of lead in the source material. Whereas, for young people, airborne lead may contribute significantly due to occupational exposure as well as exposure to smokers; for infants and young children the lead in dust and soil mostly constitutes a major exposure pathway. Most of the accumulated lead in the body is sequestered in teeth and bones causing their brittleness and weakness. The lead metal when deposited in soft body tissues may cause renal, ocular, immunological, and developmental effects.[5,6] Flora et al.[7] have reviewed comprehensively health effects of lead exposure, mechanisms involved in lead toxicity, and new advances in strategies such as chelation therapy and nano-encapsulation for the treatment of lead induced toxicity.

The conventional methods including ion-exchange, coagulation, chemical reduction, and precipitation employed for the removal of heavy metals from the contaminated water are expensive as well as inefficient.[3,4] Adsorption method, using activated carbon, has been an efficient alternative for the effective removal of heavy metals from wastewater,[8,9] but the high cost of the activated carbon limits its application at a small-scale treatment of contaminated water.

However, to reduce the cost of the adsorption process, inexpensive agricultural biowaste material such as groundnut husk,[10] rice husk,[11,12] pine needles powder,[13] guar gum biocomposite,[14] coconut waste[15] or the carbon derived from these, have earlier been used. Al-Degs et al.[16] employed natural sorbents (consisting of primary minerals, i.e., quartz and aluminosilicates and secondary minerals, i.e., calcite and dolomite) for the removal of some heavy metals. Brooks et al.[17] used alkali ash material permeable reactive barrier (AAM-PRB), a newly developed material for the removal of lead from contaminated water by batch and column experiments. Hirut et al.[18] employed low cost and eco-friendly bio-sorbent eucalyptus camaldulensis to study its capacity for removing toxic heavy metals Pb, Cd and Cr from synthetic and industrial wastewater released from textile and leather industries. Review reports on adsorption phenomenon and removal of heavy metals including Pb have also appeared in the literature.[19–24]

Low-cost clay-rich soil may be a promising sorbent material for the treatment of wastewater contaminated with heavy metals.[25] Mnasri-Ghnimi et al.[26] have used single and mixed pillared clays for the removal of some heavy metals from wastewater. In the present study, sorption behavior of Pb (II) ions over a thermally treated clay-rich soil, collected from a site (8.822634N, 40.523574E) near Gelemso town in the Western Hararghie zone of Oromia region of Ethiopia, have been studied.

Material and methods

Chemicals

Lead(II) nitrate [Pb $(NO_3)_2$, MW: 331.2, $gmol^{-1}$) and hydrochloric acid (HCl, MW: 36.5 $gmol^{-1}$) were from Blulux Laboratories. Nitric

acid (HNO_3, 98%, MW:63.10 $gmol^{-1}$), Sodium hydroxide (NaOH, 98% , MW: 40.0 $gmol^{-1}$), Sodium Chloride (NaCl, 98% MW:58.44 $gmol^{-1}$), Phenolphthalein ($C_{20}H_{14}O_4$, MW: 318.328 $gmol^{-1}$) were procured from Breckland Scientific Supplies, UK and Oxalic acid ($H_2C_2O_4$, 99.8%, MW: 90.03 $gmol^{-1}$), was from BDH Laboratories.

Sorbent material

Soils were collected from three different sites having geographical co-ordinates: (8.909331, 40.772494), (9.082266, 40.864575), (8.822634, 40.523574), situated near Bedesa, Asebe Teferi and Gelemso towns, respectively, in the western Hararghie zone of Oromia region of Ethiopia (Figure 1), and these were coded as: S1, S2 and S3, respectively. Soil sample was collected with the help of an Auger in a zigzag pattern up to 30 cm depth below the surface, from 15 different spots with one meter inter-spot separation and then mixed together in plastic bag to make a composite sample. The soil samples were dried in open air, pulverized and sieved to get particle size < 0.5 mm and then kept in moisture-free atmosphere before further use.

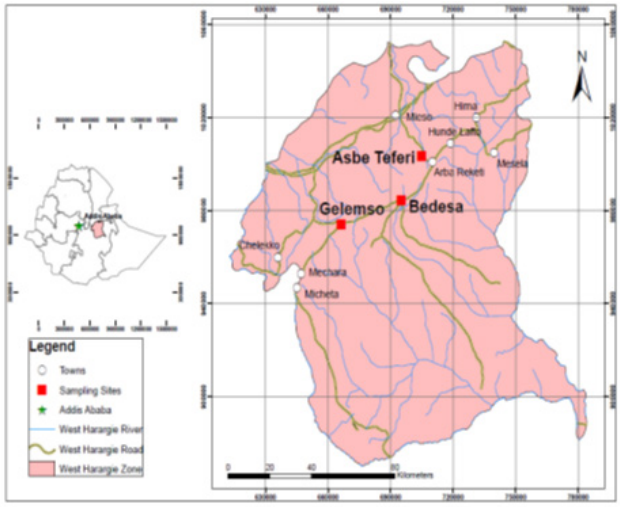

Figure 1 Three sampling sites with geographical co-ordinates: (8.909331N, 40.772494E), (9.082266N, 40.864575E), and (8.822634N, 40.523574E) near Bedesa, Asebe Teferi, and Gelemso towns, respectively in western Hararghie Zone of Oromia region of Ethiopia. *(West Harargie map under classification of Ethiopia drawn by using GIS software).*

Thermal treatment of sorbent

The optimum temperature for thermal treatment of the soil used as sorbent was determined by heating 4 g of the soil for 2 hrs, at 100^0C interval, over temperatures range: 200-900^0C and recording each time the sorption of Pb(II) ions from solution of known initial concentration.

Measurement of soil pH

To determine pH of soil, 10 g of the air-dried soil, with particle size < 2 mm, was mixed with 25 mL deionized water in a 100 mL beaker, the soil suspension was stirred for 30 minutes and then kept unstirred for 5 minutes. The pH of the clear supernatant liquid was measured using a pH meter (Model MP220, Switzerland) at ambient temperature.

Measurement of cation exchange capacity

The cation exchange capacity (CEC) of soil was determined using ammonium acetate method.[27] Typically, 100 mL 1M ammonium acetate aqueous solution (pH = 7.0) was added to 5 g soil taken in a 250 mL beaker, stirred the mixture for five minutes, and then kept as such, for overnight. The suspension was filtered through a deionized water-soaked Whatman No.1 paper. The residue was washed twice with 25 mL portion each of 1M ammonium acetate followed by washing with five successive 20 mL portion each of 10% NaCl sodium chloride solution, and the filtrate was made up to 100 mL. A blank solution was prepared similarly, where no soil was taken. The filtrate was titrated against 0.1N NaOH, and the CEC was obtained using the equation:

$$\text{CEC}\ \left(\text{meq}/100g\,\text{soil}\right)=\frac{\left(a-b\right)\times N\times 100\times mcf}{s} \quad (1)$$

Where, "a" is mL of 0.1N NaOH required for titrating the blank solution; "b" is mL of 0.1N NaOH required for titrating the sample solution; s = mass (g) of air-dried soil taken; N = normality of NaOH (0.1N), and mcf = moisture correction factor (taken as 1.00).

XRD study

An X-ray diffractometer (Brucker Axis), equipped with "Diffrac Plus 2000 Software" was employed for determining the mineral compositions of soil samples used as adsorbents, The X-ray diifraction pattern was recorded over 2θ range from 4^0 to 60^0 with 2-theta and time steps 0.020^0 and 1 second, respectively.

Specific surface area of sorbent

Specific surface areas of sorbent (Soil) was determined following Sear´s Method.[28,29] Typically, to a mixture of 1.5 g soil. and 30 g NaCl, taken in a glass beaker, was added 0.1N HCl with continuous stirring to attain pH 3.0 and the final volume was made up to 150 mL using deionized water. The mixture was titrated against 0.1M NaOH and the specific surface area of the soil was obtained using the following equation.

$$S = 32\,V - 25 \quad (2)$$

where, S = specific surface area (m^2g^{-1}) of soil, V = volume (mL) of 0.1M NaOH solution required to titrate the soil suspension from pH 4 to pH 9.

Point of zero charge (pzc) of sorbent

The pH at which a solid surface (in the absence of any specific sorption) with zero net charge is represented by *pzc*. The pzc values of sorbent was determined as described by Onyango *et al* [30]. Typically, 50 mL each of 0.01M NaCl solution was taken in separate Erlenmeyer flasks and their pH were adjusted to 2, 4, 6, 8, 10 and 12, respectively, by adding required amount of 0.1M HCl or 0.1M NaOH solution. Each solution was mixed with 0.5 g of sorbent and agitated using a shaker for 1 h and then the potential (mV) of each solution was recorded. The zero potential line intersecting the potential versus pH plot gives the ***pzc*** value on the pH Axis of the plot.

Sorption study

Sorption of Pb(II) ions onto the sorbent, in aqueous medium, was studied by batch operation method. In a typical run, a known amount of the sorbent was mixed with 100 mL of Pb(II) aqueous solution, of given concentration, in a 250 ml Erlenmeyer flask. The reaction mixture was stirred at 150 rpm for an hour prior to attaining sorption-desorption equilibrium and then centrifuged at 2500 rpm. The supernatant liquid was then analyzed for Pb(II) ion concentration using an atomic absorption spectrophotometer (BUCK) and adopting 3111A standard procedure[31] and measuring the absorbance at 217 nm, slit width 0.7 nm, lamp current 5.0 mA, detection limit 0.01 mg/L. Percentage removal of Pb(II) was calculated using the equation:

$$\text{Percent removal} = \left[\left(C_0 - C_e\right) / C_0\right] x100 \quad (3)$$

Citation: Fikre A, Kebede T, Yadav OP. Equilibrium and kinetic behavior of Pb(II) ions sorption onto thermally treated clay-rich soil collected near Gelemso town of Oromia region in Ethiopia. *J Anal Pharm Res.* 2022;11(2):79–87. DOI: 10.15406/japlr.2022.11.00405

where, C_0 and Ce are initial and equilibrium concentrations of Cr(VI) ions (in mgL^{-1}), respectively. Sorption capacity (q_t) of the sorbent for Pb(II) ions, at the given reaction time t, was calculated using the equation:

$$q_t = \frac{(C_0 - C_t)V}{m} \quad (4)$$

Where: C_o and C_t are metal ions concentrations (mg/L) in the initial stage and at time, respectively; V is volume of the metal ions solution in liter; m is mass (g) of the sorbent taken, and q_t is sorption capacity (mg g^{-1}).

Statistical analysis

The sorption data generated was analyzed using one-way ANOVA, LSD test and regression analysis and graphs were generated using the software package STATISTICA (released 8.0) for WINDOWS.

Results and discussion

Characteristics of sorbent

Clay percent, pH and cation exchange capacity (CEC) of three soil samples collected from different sites are given in Table 1.

Table 1 Some characteristic properties of three soils collected from different sites of western Hararghie zone of Oromia region of Ethiopia

Soil sample site	Soil Code	Clay Content (%)	Soil pH	CEC/ meq/100gsoil)
Bedesa	S1	9.08	6.68	57.4
Asebe Teferi	S2	21.08	7.22	42.3
Gelemso	S3	43.02	8.73	59.2

*Bedesa (8.909331N, 40.772494E); Asebe Teferi (9.082266N, 40.864575E), and Gelemso (8.822634N, 40.523574E) in Western Hararghie zone of Oromia region of Ethiopia.

Since the soil sample labeled as S3 (collected from Gelemso) has highest clay content as well as cation exchange capacity, among the three collected soil samples, therefore, it was selected as the sorbent in the subsequent part of the present study.

Thermal treatment of sorbent

To optimize the temperature for thermal treatment of sorbent, soil (S3) was heated from 200 to 900^0 C in a step of 100 ^{0}C. The plot of percent removal of Pb(II) ions as a function of thermal treatment temperature, using Pb(II) ions initial concentration 30 mg/L, sorbent dose 10 gL^{-1}, pH 5, and sorbate-sorbent contact time 6 hrs, is presented in Figure 2. Percent removal of Pb(II) ions upon varying treatment temperature 200^0C to 400^0C only slightly increased from 95 to 97 %, remained constant over 400 to 500^0C, and beyond that, removal of Pb(II) ions gradually decreased. Such decrease in Pb(II) ions removal at higher temperatures may be due to agglomeration of soil (sorbent) particles causing their decreased specific surface area.[32] Thus, 400^0C was taken as the optimum temperature for the thermal treatment of the sorbent.

Specific surface area of sorbent

Specific surface areas of thermally treated soil sorbents (S3), determined using Sears' method described in Section 2.3.5, was 32.4 m^2/g.

XRD analysis

A typical XRD pattern of untreated soil (S3) is shown in Figure 3 and the percentage composition of various minerals present in the soil are recorded in Table 2. Whereas, Kaolinite [$Al_2Si_2O_5(OH)_4$] with highest concentration (52.6%) was found to be the major constituent of the selected soil, the level of Vermiculite [$Mg_3Si_4O_{10}(OH)_2$] with 3.3% concentration, was the lowest. The other two minerals: Quartz (SiO_2) and Phosphosiderite [$(FePO_4(H_2O)_2$] present in the soil were 24.5% and 19.6%, respectively.

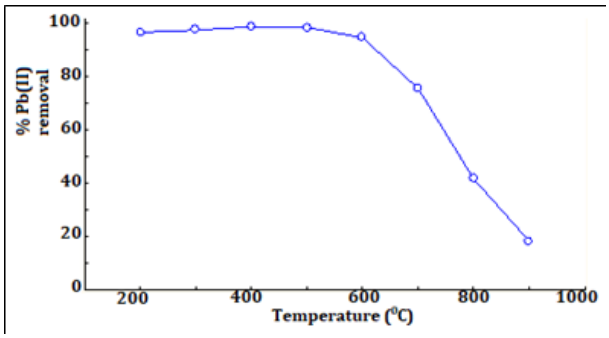

Figure 2 Percent removal of Pb(II) ions from aqueous solution as a function of thermal treatment temperature of soil (sorbent dose =10 gL^{-1}, pH = 5, Pb(II) ions concentration: 30 mgL^{-1}, contact time = 6 hrs).

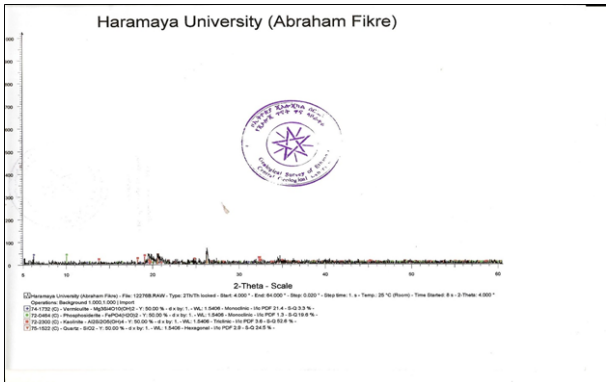

Figure 3 The X-ray diffraction (XRD) pattern of untreated soil sample (S3).

Table 2 Percentage composition of various minerals present in untreated soil sample (S3) as obtained from XRD analysis

Mineral	Chemical Formula	Percentage (%)
Quartz	SiO_2	24.5
Vermiculite	$Mg_3Si_4O_{10}(OH)_2$	3.3
Kaolinite	$Al_2Si_2O_5(OH)_4$	52.6
Phosphosiderite	$FePO_4(H_2O)_2$	19.6

Point of zero charge (pzc) of soil (sorbent)

The plot of electrical potential (millivolts) as a function of pH of the solution is shown Figure 4. The *pzc* of the soil (sorbent) obtainable from the pH value that corresponds to zero electrical potential on the plot was found to be 4.6. There always exists a relationship between pzc value of the sorbent and its sorption capacity. Whereas, the sorption of a cationic specie at a pH higher than the *pzc* of the sorbent will be favoured, an anion's sorption, on the other hand, will be favored at pH lower than the *pzc* of sorbent.[33]

Effects of parameters on metal ions sorption

Various parameters that may affect the extent of metal ions sorption onto the sorbent include: sorbent amount, pH of solution, metal ions initial concentration, and sorbate-sorbent contact time.

Effect of sorbent amount

Percentage removal of Pb(II) ions from solution, and the amount of Pb(II) ions sorbed per unit mass of the sorbent q_e (mgg^{-1}) at sorbate-

sorbent contact time 3 hrs, as a function of sorbent dose using initial concentration of Pb(II) = 20 mgL^{-1}, solution pH = 5, are presented in Figure 5. Upon increasing sorbent concentration from 1 to 4 gm per 100 mL the percent removal of Pb(II) slightly increases, and at still higher sorbent load it becomes constant. The initial increase in the sorption of Pb(II) ions upon increasing the sorbent dose may be ascribed to enhanced availability of binding sites on the sorbent per sorbate ion/molecule.[34] However, beyond the optimum value 4% (w/v) of sorbent dose, no additional removal of the sorbate was recorded indicating that the full sorption potential of the sorbent is being exploited.[35] Further, with Pb(II) ions fixed initial concentration ($20mgL^{-1}$), the sorption capacity i.e. the amount of Pb(II) ions sorbed per unit mass of the sorbent q_e (mgg^{-1}) at 3 hrs, decreased upon increasing sorbent dose.

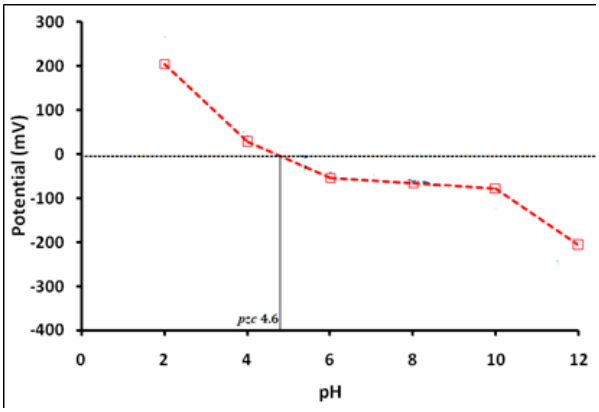

Figure 4 Plot of electrical potential (millivolts) as a function of pH for untreated and thermally treated soils collected from Gelemso (S3).

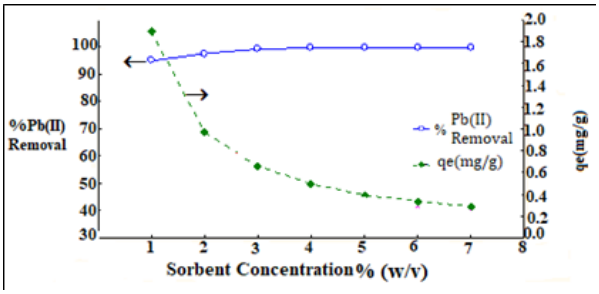

Figure 5 Percentage removal of Pb(II) ions and amount of Pb(II) sorbed per unit mass of the sorbent at equilibrium, q_e (mgg^{-1}) as a function of sorbent dose (gL^{-1}) (Pb(II) ions Initial concentration = 20 mgL^{-1}, solution pH = 5, and sorbate-sorbent, contact time 3 hrs).

Effect of pH

The plot of % removal of Pb(II) ions at 2 hours, as a function of pH using Pb(II) ions initial concentration = 40 mg/L and sorbent dose 4 g per 100 mL is shown in Figure 5. Solution pH plays an important role in the sorption of the sorbate [(Pb(II) ions] due to its influence on the surface properties of the sorbent as well as on the ionic forms of the sorbate in solutions[36] resulting variation in sorbate-sorbent interaction and hence the extent of the sorbate removal. For instance, at a pH < pzc (4.6) of sorbent, clay particles present in the soil interact with water in aqueous solution and acquire positive charge due to the formation of an aqua complex according to the following chemical reaction.[37]

$$\underset{\text{(Clay)}}{-MOH} + H - OH \xrightarrow{H^+} \underset{\text{(Aqua Complex)}}{M - OH_2^+} + OH^-$$

Thus, the observed poor % removal of Pb(II) ions at low pH (Figure 6) can be due to the ion-ion repulsion due to positive charge both on the sorbent as well as the Pb(II) ions. However, at a pH >pzc, the sorbent's surface becomes negatively charged as per the following chemical reactions[38] favoring closer approach of the oppositely charged sorbent and the sorbate and thus the more % removal of the Pb(II) from the aqueous solution (Figure 6).

$$\underset{\text{Zwitter Ion at } pzc}{-MOH^{\pm}} + OH^- \xrightarrow{(pH > pzc)} \underset{\text{Negatively Charged Clay}}{-MO^-} + H_2O$$

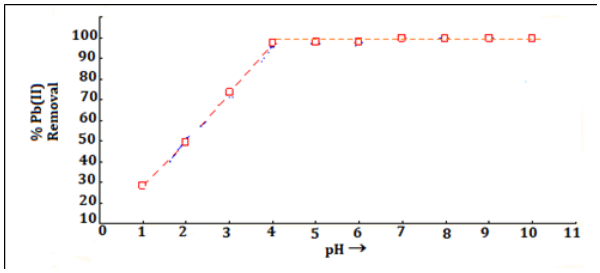

Figure 6 Percent Pb(II) ions removal as a function of pH at 2 hours using Pb(II) ions initial concentration = 40 mg/L, adsorption dose = 4% (w/v).

Upon raising pH from 1 to 4, the removal of Pb(II) ions from aqueous solution increases due to diminishing positive charge on the sorbent surface at higher pH resulting in an enhanced sorbate -sorbent attraction. However, the observed constant percent removal of Pb(II) above pH 4, may be attributed to the saturation of by the binding sites on the sorbent as well as the attainment of sorption ⇌ desorption equilibrium.

Effect of contact time

In order to optimize the time required for maximum sorption of Pb(II) ions onto the sorbent, a plot of amount of Pb(II) ions sorbed per gram of sorbent, q (mgg^{-1}), as a function of sorbate-sorbent contact time, using a fixed Pb(II) ions initial concentration 100 mgL^{-1}; solution pH 4, and sorbent load 4% (w/v), was drawn (Figure 7). It was found that the metal ion sorption increased with increasing contact time till 120 min and beyond that it became constant. The observed increase in sorption of Pb(II) ions upto120 min (the optimum time), is because of higher rate of sorption compared to the desorption of the sorbate, and the subsequent constant metal ions sorption till 270 min is attributed to the attainment of the sorption desorption equilibrium. The amount of sorbate i.e. Pb(II)]ions, sorbed at the equilibrium time gives the maximum sorption capacity of the sorbent under the given condition.

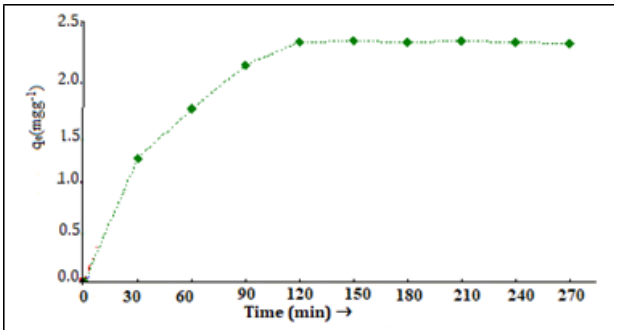

Figure 7 Plot of amount of Pb(II) ions sorbed per gram of sorbent, q (mgg^{-1}) versus sorbate-sorbent contact time. [Pb(II) ions initial concentration =100 mgL^{-1}; solution pH = 4, and sorbent load=4 % (w/v).

Citation: Fikre A, Kebede T, Yadav OP. Equilibrium and kinetic behavior of Pb(II) ions sorption onto thermally treated clay-rich soil collected near Gelemso town of Oromia region in Ethiopia. *J Anal Pharm Res.* 2022;11(2):79–87. DOI: 10.15406/japlr.2022.11.00405

Effects of sorbate initial concentration

A plot of sorption capacity [amount of sorbate sorbed per gram of the sorbent, q_e (mgg^{-1})] as a function of sorbate initial concentration (mgL^{-1}) at specified conditions is shown in Figure 8. The sorption capacity was found increasing linearly, with the initial concentration of sorbate i.e, Pb(II) ions upto 100 mgL^{-1}.

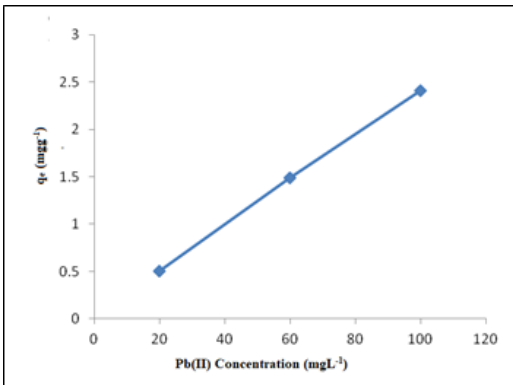

Figure 8 Plot of sorption capacity [amount of (Pb(II) ions sorbed per gram of the sorbent, q_e (mgg^{-1})] as a function of Pb(II) ions initial concentration (mgL^{-1}) (solution pH = 4, sorbent load=4 % (w/v), and contact time 120 min).

Langmuir sorption isotherm

In Langmuir's sorption treatment.[39] It is assumed that a: sorbent surface is homogeneous; b: all active sites at the sorbent surface are equivalent; c: there is a monolayer coverage by the sorbate molecules at the sorbent surface, and d: there is no interaction between the sorbate molecules at adjacent binding sites. Accordingly, the linear form of the Langmuir sorption isotherm is given by the equation:

$$c_e / q_e = 1/(Q_o K_L) + (1/Q_o)c_e \quad (5)$$

Where, c_e is the equilibrium concentration of sorbate (mgL^{-1}) in the solution, q_e is the amount of sorbate sorbed per unit mass of the sorbent at equilibrium (mgg^{-1}); Q_o is the amount of the sorbate sorbed per unit mass of sorbent (mgg^{-1}) to form a monolayer, and K_L is the Langmuir constant related to the affinity of binding sites (mg^{-1}) and is a measure of the energy of sorption. The Langmuir constants Q_o and K_L obtained from the intercept and slope of linear plot of c_e/q_e versus c_e (Figure 9) and are given in Table 3 along with the correlation coefficient (R^2). The obtained high value of Langmuir parameter, K_L =10.57 $(mg)^{-1}$, suggests strong interaction of Pb(II) ions with the sorbent's binding sites due to coulombic ion-ion interaction suggesting the involvement of a chemisorption process. Further, the value of parameter Q_o = 2.215 (mgg^{-1}) obtained, suggests a high intensity of Pb(II) ion sorption on the sorbent.

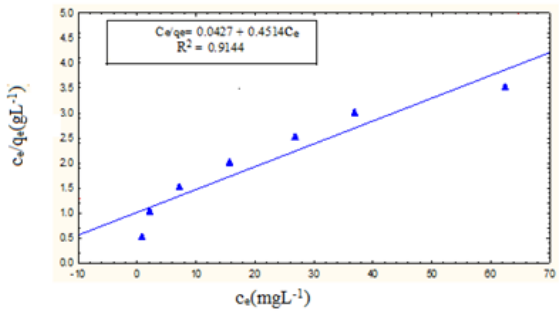

Figure 9 Langmuir adsorption isotherm i.e. a plot of C_e/q_e versus C_e [Pb(II) ions initial concentration = 20 mg L^{-1}; pH = 4.5; sorbate-sorbent contact time = 120 min].

Table 3 Parameters of sorption isotherm models

Langmuir isotherm	Freundlich isotherm	Temkin isotherm
Ce/qe = 1/(QoKL)+(1/Qo)Ce	ln qe = ln KF + (1/n) lnCe	qe = (RT/b)lnA + (RT/b)lnce Where, RT/b =B
R2 = 0.9144	R2 = 0.9894	B= 0.3809 (L/g)
$C_e/q_e = 1/(Q_oK_L)+(1/Q_o)C_e$	$\ln q_e = \ln K_F + (1/n)\ln C_e$	$q_e = (RT/b)\ln A + (RT/b)\ln c_e$ Where, RT/b =B
R^2 = 0.9144	R^2 = 0.9894	B= 0.3809 (L/g)

Freundlich sorption isotherm

Freundlich sorption model[40] assumes specific interactions of sorbate molecules/ions with the heterogeneous sites at the sorbent surface with varied affinities and also allows multilayer sorption. This model is more general than the Langmuir isotherm, since it does not assume a homogenous surface or constant sorption potential. It also assumes that the stronger binding sites are occupied first and their binding strength decreases with the increasing degree of site occupation. The Freundlich equation that describes sorbate-sorbent equilibrium is expressed as:

$$q_e = K_f . c_e^{1/n} \quad (6)$$

Where, q_e represents the amount of solute retained by the sorbent ($mg\ g^{-1}$), c_e (mgL^{-1}) is the solute equilibrium concentration in solution, K_f(Lmg^{-1}) is related to the sorption capacity of the sorbent or bonding energy for a given sorbate - sorbent system at a given temperature and can be defined as the sorption or distribution coefficient representing the quantity of sobate sorbed for a unit equilibrium concentration, and '*n*' is the dimensionless reaction order commonly less than one. It is also related to the sorption intensity or surface heterogeneity of the system. Freundlich model can be expressed by a linear form of equation.[41]

$$\log q_e = \log K_F + (1/n)\log c_e \quad (7)$$

The values of Freundlich parameters K_F and n, obtainable from the intercept and the slope, respectively, of the linear plot of $\log q_e$ versus $\ln c_e$ (Figure 10), are given in Table 3. The values of K_F and 'n' thus obtained were 1.906 and 2.17, respectively. Since the value of "n" lies between 0 and 1, it indicates that the studied clay-rich soil can effectively adsorb the Pb(II) ions and thus can enable their removal from aqueous solution. The observed higher correlation coefficient (R^2) for Freundlich model (0.9894) compared to that for Langmuir model (0.9144) suggests that the former model fits better for the studied sorbate-sorbent system.

Temkin sorption isotherm

The sorption equilibrium data was also analyzed according to Temkin isotherm.[42,43] The linear form of the Temkin isotherm can be expressed as:

$$q_e = (RT/b)\ln c_e + (RT/b)\ln A \quad (8)$$

Where, q_e represents the amount of solute retained by the sorbent ($mg\ g^{-1}$), c_e (mgL^{-1}) is the sorbate equilibrium concentration in solution, and RT/b=B. The parameters A and B determined from the intercept and slope of the plot q_e versus $\ln c_e$ (Figure 11), are given, along with correlation co-efficient (R^2), in Table 3. The correlation co-efficient for Temkin isotherm plot is lower than that for the Freundlich

Citation: Fikre A, Kebede T, Yadav OP. Equilibrium and kinetic behavior of Pb(II) ions sorption onto thermally treated clay-rich soil collected near Gelemso town of Oromia region in Ethiopia. *J Anal Pharm Res.* 2022;11(2):79–87. DOI: 10.15406/japlr.2022.11.00405

Isotherm but higher compared to the Langmuir Isotherm value Figure 11 A.

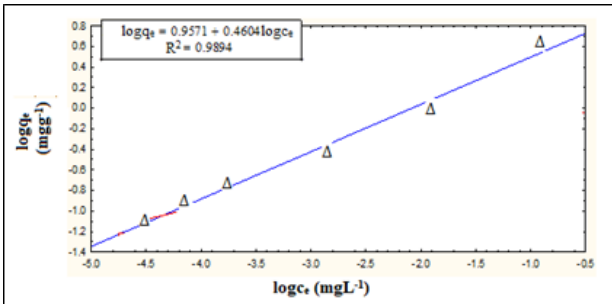

Figure 10 Freundlich isotherm i.e. a plot of log q_e versus log c_e for sorption of Pb(II) ions onto thermally treated clay-rich soil S3 [Pb(II) ions initial concentration = 20 mgL^{-1}; pH = 4.5 ; sorbate-sorbent contact time = 120 min].

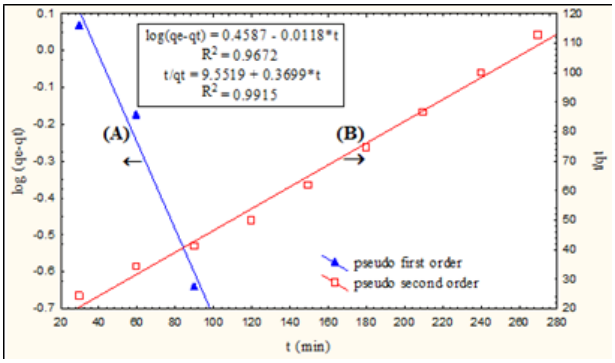

Figure 10A *(A)* Plot of log(q_e - q_t) versus contact time t (min), and *(B):* Plot of t/q_t versus contact time t (min) [Pb(II) ions initial concentration 100mgL^{-1}; sorbent load = 4 gL^{-1},pH = 5).

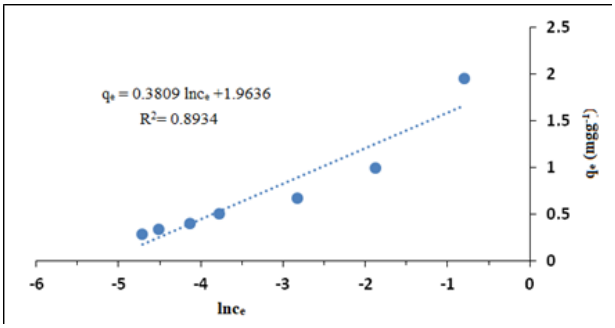

Figure 11 Temkin sorption isotherm i.e. a plot of q_e as a function lnc

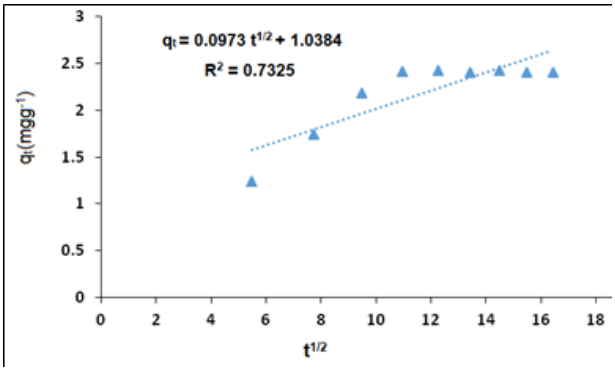

Figure 11(A) The plot of amount of Pb(II) sorbed per gram of sorbent, q_t(mgg^{-1}) as a function of $t^{1/2}$ (Pb(II) ions initial concentration: 100 mgL^{-1}, sorbent dose = 4 gL^{-1}, pH = 5).

Sorption kinetic study

Three sequential steps involved during the sorption of a solute onto a sorbent are: 1. Film diffusion, where sorbate travels from the bulk towards the external surface of the sorbent; 2. Particle diffusion, where sorbate travels within the pores of the sorbent, and 3. Sorption of the sorbate on the interior surface of the sorbent.[44] The observed sorption data were analyzed in terms of five different kinetic models as described in the following sections.

Pseudo-first-order kinetic model

The linear form of the *pseudo-first-order* sorption rate equation, can be written as:

$$ln(q_e - q_t) = lnq_e - k_1 t \quad (9)$$

$$\text{or } log\ (q_e - q_t) = logq_e - (k_1 / 2.303)t \quad (10)$$

Where, q_e and q_t are the theoretical sorption efficiency (amount of the sorbate i.e. Pb(II) ions, sorbed per gram of the sorbent (mgg^{-1}) at equilibrium, and at time 't', respectively; k_1 is the sorption rate constant (min^{-1}). The values of q_e and k_1, obtainable from the intercept and the slope, respectively, of the plot between log $(q_e - q_t)$ versus 't' (Fig. 10A), are given along with the correlation coefficient (R^2), in Table 4. The lower value of the calculated sorption efficiency q_e (1.66 mgg^{-1}) compared to the experimental q_e (2.41mgg^{-1}), suggests the poor applicability of the *pseudo-first-order* kinetic model to the studied sorbate-sorbent system.

Table 4 Summary results of sorption kinetic models parameters

Experimental qe	Sorption Kinetic Model	Kinetic Parameters
2.41mgg-1	Pseudo-First-Order Kinetic Model log (qe – qt) = logqe – (k1/2.303)t	qe = 1.29 mgg-1 k1 = 2.72x10-2 min-1 R2 = 0.9670
2.41mgg-1	Pseudo-Second-Order Kinetic Model t/qt = 1/(k2.qe2) + (1/qe).t	k2 = 1.44x10-2 min-1 R2 = 0.9915
2.41mgg-1	Intra-particle diffusion Model qt = kit1/2+C	ki = 9.73x10-2 min-1 C=1.0384 R2 = 0.7325
2.41mgg-1	Boyd Kinetic Model Bt = -0.4977 – ln(1-F)	R2 = 0.8510
2.41mgg-1	The Elovich Model qt = (1/β)lnt + (1/β)ln (αβ)	α = 3.72x10-2 min-1 β = 3.81 R2 = 0.9914

Pseudo-second-order kinetic model

The *pseudo-second-order* sorption rate can be represented by the linear form of equation:

$$t / q_t = 1/\left(k_2.q_e^2\right) + \left(1/q_e\right).t \quad (11)$$

Where, k_2 is *pseudo-second order* sorption rate constant (g/mg min); q_t and q_e are amount of sorbate i.e Pb (II), sorbed per gram of the sorbent (mg/g) at contact time t, *and* at equilibrium, respectively. The values of q_e, and k_2, obtainable from the slope and intercept, respectively, of the linear plot of t/q_t versus contact time t (Fig. 10B), are presented given in Table 4, along with the correlation coefficient

(R^2). The calculated q_e value (2.70 mgg^{-1}) close to the experimentally obtained q_e (2.41mgg^{-1}), and high correlation coefficient R^2 =0.9910 imply that the sorption of Pb(II) onto the studied sorbent fits well in the pseudo-second-order sorption model.

Intra-particle diffusion model

Intra-particle diffusion model due to[45] for a sorption system is generally expressed in the linear form of equation:

$$q_t = k_i t^{1/2} + C \quad (12)$$

Where, q_t is quantity of solute sorbed at the sorbent (mgg^{-1}) at time t and k_i is intra-particle diffusion rate constant (mg/g $min^{1/2}$). The plot of q_t as a function of $t^{1/2}$ (using Pb(II) initial concentration 100 mgL^{-1}, sorbent dose = 4 gL^{-1}, pH = 5) is shown in in Figure 11. The values of k_i and C were obtained from the slope and intercept, respectively, of q_t versus $t^{1/2}$ plot and are given in Table 4. Larger the value of C, greater is the boundary layer effect. For pure intra-particle diffusion to take place, the plot of q_t versus $t^{1/2}$ should be linear, passing through the origin. However, if the plot shows multilinearity, as is observed in the present case, it indicates that more than one step is involved in the sorption process i.e the sorption may be controlled by the combination of film and intraparticle diffusion[46] Thus in the present case, it can be concluded that both the surface sorption as well as the intra-particle diffusion may be concurrently operating during the sorption of Pb(II) ions on the studied clay-rich soil sorbent (S-3). The intra-particle diffusion rate constant (k_i = 9.73x10^{-2} min^{-1}) was found to be higher than the sorption kinetic rate constants for pseudo -first- order (k_1=2.72x10^{-2} min^{-1}) as well as pseudo-second-order (k_2=1.44x10^{-2} min^{-1}).

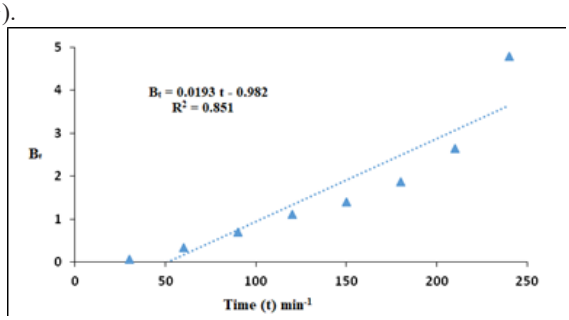

Figure 12 Plot of B_t as a function of sorbate-sorbent contact time t(Pb(II) ions initial concentration: 100 mgL^{-1}, sorbent dose = 4 gL^{-1}, pH = 5).

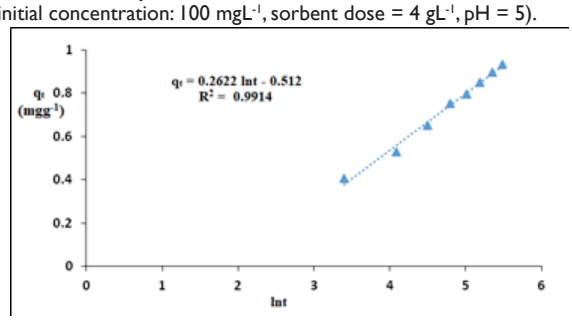

Figure 13 Plot of q_t(mgg^{-1})as a function of lnt [(Pb(II) ions initial concentration: 100 mgL^{-1}, sorbe nt dose = 4 gL^{-1}, pH = 5].

The Boyd kinetic model

To determine the rate-controlling step involved in the sorption process, the observed data were also analyzed in terms of Boyd kinetic model[47] represented by the following equation:

$$B_t = -0.4977 - ln(1-F) \quad (13)$$

Where, F represents the fraction of solute sorbed at any time, t (min) and is given by F = q_t/q_∞. Where, q_t, and q_∞ represent amount of the sorbate sorbed per gram of the sorbent (mg g^{-1}) at time t (min) and at infinite time, respectively. The plot of B_t as a function of time t (min) is shown in Figure 12. The linearity test of B_t vs. time plot was used to distinguish between the film diffusion- and particle diffusion-controlled sorptions. The linear plot of B_t versus. time t passing through the origin, will suggest that the sorption rate is governed by particle diffusion mechanism otherwise the same is considered to be governed by film diffusion[48] Since for the present sorbate-sorbent system the B_t versus time linear plot does not pass through the origin, it suggests that the sorption rate of Pb(II) ions onto the studied sorbent is controlled by film diffusion.

The Elovich kinetic model

The Elovich model of sorption kinetics[49] can be represented by the equation: (βq_t)

$$dq_t / dt = \alpha e^{-(\beta q t)} \quad (14)$$

The integration of the Elovich rate equation using the same boundary conditions as for the pseudo-first-order, and pseudo second-order equations yields the linear form of Elovich Equation represented by:

$$q_t = (1/\beta)\ln t + (1/\beta)\ln(\alpha\beta) \quad (15)$$

Where, α is the initial sorption rate (mg/g min) and the parameter β (g/mg) is related to the extent of surface coverage and activation energy for chemisorptions.

The sorption kinetic constants α, and β, obtainable from the intercept and the slope of the linear plot of q_t versus lnt (Fig.13) are given alongwith correlation coefficient (R^2) in Table 4. The kinetic rate constant (α = 3.72x10^{-2} min^{-1}) predicted by the Elovich equation is higher compared to sorption rates obtained for the pseudo -first-order (k_1=2.72x10^{-2} min^{-1}) and pseudo-second-order (k_2=1.44x10^{-2} min^{-1}) kinetic models. The correlation co-efficient R^2 (= 0.9914) for Elovich equation is almost equal to that for the pseudo second order equation but higher than that for the other three studied kinedic models. Although Elovich Equation does not provide any mechanistic evidence, yet it has proved suitable for kinetic study of highly heterogeneous systems such as the present sorption of Pb (II) onto the clay-rich soil sorbent (S3).

Conclusion

The effects of sorbent dose, contact time, pH, and sorbate initial concentration on the sorption of Pb(II) ions on a clay-rich thermally treated soil, collected from a site near Gelemso town in Western Hararghie Zone of Oromia region of Ethiopia, have been studied using batch experiments. The sorption data were analyzed in terms of Langmuir, Freundlich and Temkin isotherms. The Freundlich sorption model was demonstrated to provide the best correlation for the studied sorbate-sorbent system indicating the existence of heterogeneous functional groups in the sorbent for interacting with Pb(II) ions. As high as 95% Pb(II) ions could be removed from their 20 mg/L^{-1} aqueous solution within 3 hrs using optimized pH and sorbent doze. Among the five kinetic models applied for the analysis of sorption data, the pseudo-second-order model, with highest R^2 (= 0.9910), provided the best correlation with the experimental data. The results of present investigation show that studied clay-rich soil with sorption capacity 2.22 mgg^{-1} can be used as a low-cost sorbent for the treatment of wastewater contaminated with low levels of Pb(II) ions.

Acknowledgements

The authors thankfully acknowledge the receipt of financial

grants from the Ministry of Education, Ethiopia, through Haramaya University, for carrying out this research work and also appreciate the co-operation received from the Geosciences Laboratory of Geological Survey of Ethiopia, Addis Ababa, for their providing X-ray analysis facility.

Conflicts of interest

The authors declare that there is no conflict of interest.

References

1. Masindi V, Muedi K. *Environmental contamination by heavy metals*. In: Heavy Metals. *Intech Open.* 2018.
2. Ukaogo PO, Ewuzie U, OnwukaC V. 21-Environmental pollution: causes, effects, and the remedies, Eds: Pankaj Chowdhary et al. Microorganisms for Sustainable Environment and Health. Elsevier. 2020. p. 419–429.
3. Iqbal M, Saeed A, Akhtar N. Petiolar felt-sheath of palm: a new biosorbent for the removal of heavy metals from contaminated water *Bioresour Technol.* 2002;81:151–153.
4. Ali I, Asim M, Khan TA. Low cost adsorbents for removal of organic pollutants from wastewater. *J Environ Manage.* 2012;113:170–183.
5. Todd AC, Wetmur JG, Moline JM, et al. Unraveling the chronic toxicity of lead: an essential priority for environmental health. *J Environ Health Perspect.* 1996;104:141–146.
6. O Connell DW, O Dwyer, TF. Heavy metals adsorbents prepared from the modification of cellulose: a review. *Biosource* Technology. 2008; 6709–6724.
7. Flora G, Gupta D Tewari A. Toxicity of lead: A review with recent updates. *Interdiscip Toxicol*. 2012;5:47–58.
8. Selvi K, Pattabhi S, Kadirvelu K. Removal of Cr (VI) from aqueous solution by adsorption on to activated carbon. *Bioresource Technol.* 2001;80:87–89.
9. Karthikeyan T, Rajgopal S, Miranda L R. Chromium (VI) adsorption from aqueous solution by Hevea brasilinesis sawdust activated carbon. *J Hazard Mater.* 2005;124:192–199.
10. Periyasamy K, Srinivasan K, Murugan P K. Studies on chromium (VI) removal by activated groundnut husk carbon. *Indian J Environ Health,* 1991;33:433–439.
11. Singh SR, Singh A P. Treatment of water containing chromium (VI) using rice husk carbon as a new low cost adsorbent. *Int J Environ Res.* 2012;6:917–924.
12. Hegazi HA. Removal of heavy metals from wastewater using agricultural and industrial wastes as adsorbents. *HBRC Journal.* 2013;9:276–282.
13. Hadjmohammadi MR, Salary M, Biparva P. Removal of Cr(VI) from aqueous solutions using pine needles powder as a biosorbent. *J Appl Sci Environ Sanit.* 2011;6:1–13.
14. Khan TA, Nazir M, Ali I, et al. Removal of chromium (VI) from aqueous solution using guar gum-nano zinc oxide biocomposite adsorbent. *Arabian J Chem*. 2013;39.
15. Rahim ARA, Iswarya Johari K, Shehzad N, et al. Conversion of coconut waste into cost effective adsorbent for Cu(II) and Ni(II) removal from aqueous solutions. *Environ Eng Res.* 2021;26:200250.
16. Al-Degs YS, El-Barghouthi M I, Issa AA, et al. Sorption of Zn(II), Pb(II), and Co(II) using natural sorbents: equilibrium and kinetic studies. *Water Res*. 2006;40:2645–2658.
17. Brooks R M, Bahadory M, Tovia F, et al. Removal of Lead from Contaminated Water. *Int J Soil Sediment and Water.*2010;3:1–13.
18. Hirut G, Abraha G, Libargachew D. Removal of heavy metals from aqueous solutions using *Eucalyptus Camaldulensis*: An alternate low cost adsorbent. *Cogent Chemistry.* 2020;6:1
19. Kaushal A, Singh SK. Adsorption phenomenon and its application in removal of lead from waste water: a review. *Int J Hydro.* 2017;1:38–47.
20. Shaikh TMA. Adsorption of Pb(II) from wastewater by natural and synthetic adsorbents. *Biointerface Research in Applied Chemistry*. 2020:10:6522–6539.
21. Oladoye PO. Natural, low-cost adsorbents for toxic Pb(II) ion sequestration from (waste)water: A state-of-the-art review. *Chemosphere*. 2021;287:132130.
22. Bilal M, Ihsanullah I, Younas M, et al. Recent advances in applications of low-cost adsorbents for the removal of heavy metals from water: A ritical review. *Separ and Purific Technol.* 2021;278:119510.
23. Kamal B, Rafey A. A mini review of treatment methods for lead removal from wastewater. *Int J Envir Anal Chem.* 2021.
24. Velusamy S, Roy A, undaram S, et al. A Review on Heavy Metal Ions and Containing Dyes Removal Through Graphene Oxide-Based Adsorption Strategies for Textile Wastewater Treatment. *Chem Rec.* 2021;21:1570–1610.
25. Bhattacharya GK, Gupta SS. Adsorption of chromium(VI) from water by clays. *Ind Eng Chem Res.* 2006;45:7232–7240.
26. Mnasri-Ghnimi S, Frini-Srasra N. Removal of heavy metals from aqueous solutions by adsorption using single and mixed pillared clays. *Applied Clay Science*. 2019;179:105151.
27. Chapman HD. *Cation-Exchange Capacity, Chapt 57*. Agronomy Monographs, Ed: A G Norman, 1965.
28. Sears GW. Determination of specific surface area of colloidal silica by titration with sodium hydroxide. *J Analyt Chem*. 1956;28:1981–1983.
29. Mekhamer WK. The colloidal stability of raw bentonite deformed mechanically by ultrasound. *J Saudi Chem Soc*. 2010;14:301–306.
30. Onyango MS, Kojima Y, Aoyi O, et al. Adsorption equilibrium modeling and solution chemistry dependence of fluoride removal from water by trivalent cation exchange zeoute. *J Colloid Interface Sci.* 2004;279:341–350.
31. APHA (American public Health Association), 2005. *Standard Methods for the Examination of Water and Wastewater*. 7th edn. Washington DC.
32. Aytas, S, Yurtlu M, Donat R. Adsorption characterstic of U(VI) ion onto thermally activated bentonite. *J Hazard Mater.* 2009;172:667–674.
33. Saifuddin NM, Palanisamy K. Removal of Heavy metal from industrial waste using chitosan coated oil palm shell charcoal. *J Biotechnology*. 2005;8:43–53.
34. Kumar KV, Sivanesan S. Prediction of optimum sorption isotherm: Comparison of linear and non-linear method. *J Hazard Mater.* 2005;*1*26:198–201.
35. Gupta SS, Bhattacharyya KG. Adsorption of Ni(II) on Clays. *J Colloid Interface Sci.* 2006;295:21–32.
36. Olu-Owolabi BI, Popoola DB, Unuabonah EI. Removal of Cu^{+2} and Cd^{+2} from aqueous solution by bentonite clay modified with mixture of goethite and humic Acid. *Water, Air & Soil Pollution*. 2010;211:459–474.
37. Mathialagan T, Vararaghavan T. Adsorption of cadmium from aqueous solutions by perlite. *J Hazard Mater.* 2002;94;291–303.
38. Dimitrova SV. Metal Sorption on Blast-Furnace Slag. *J Water Research*. 1996;30:228–232.
39. Langmuir I. The arrangement of electrons in atoms and Molecules. *J Amer Chem Soc*. 1919;41:868–934.

40. Freundlich H. Adsorption in Solution. *Zeitschrift* für *Physikalische Chemie*, 1906;57:384–470.

41. Altin O, Ozbelge HO, Dogu T. Use of general purpose adsorption isotherms for heavy metal–clay mineral interactions. *J Colloid Interface Sci.* 1998;198:130–140.

42. Ozacar M. Equilibrium and kinetic modelling of adsorption of phosphorus on calcined alunite. *Adsorption*. 2003;9:125–132.

43. Ornek A, Ozakar M, Sengil IA. Adsorption of lead onto formaldehyde or sulphuric acid treated acron waste : Equilibrium and kinetic studies. *Biochem Eng Journal.* 2007;37:192–200.

44. Tan, IAW, Hameed BH. Adsorption isotherms, kinetics, thermodynamics, and desorption of activated carbon derived from oil palm empty fruit bunch. *J Appl Sci.* 2010;10:2565–2571.

45. Weber WJ, Morris JC. Kinetics of adsorption on carbon from solutions. *J Sanitary Eng. Div.* 1963;89:31–60.

46. Chio CP, Lin MC, Liao CM. Low-cost farmed shrimp shells could remove arsenic from aqueous solutions kinetically. *J Hazard. Mater.* 2009;171:859–864.

47. Boyd, GE, Adamson AW, Myres LS. Kinetics of ionic exchange adsorption processes. *J Amer Chem. Soc*. 1947;69:2836–2848.

48. Mahmood T, Din SU, Naeem A, et al. Kinetics, equilibrium and thermodynamics studies of arsenate adsorption from aqueous solution onto iron hydroxide. *J Indus Eng Chem.* 2014;25:3234–3242.

49. Özacar M, Sengil IA. A kinetic study of metal complex dye sorption onto pine sawdust. *Process Bioch.* 2005;40:565–572.

Citation: Fikre A, Kebede T, Yadav OP. Equilibrium and kinetic behavior of Pb(II) ions sorption onto thermally treated clay-rich soil collected near Gelemso town of Oromia region in Ethiopia. *J Anal Pharm Res.* 2022;11(2):79–87. DOI: 10.15406/japlr.2022.11.00405